Original Article | Gastrointestinal Imaging

eISSN 2005-8330
https://doi.org/10.3348/kjr.2023.0521
Korean J Radiol 2023;24(12):1232-1240

Korean Journal of Radiology
KJR

Large Duct Pancreatic Ductal Adenocarcinoma: A Morphological Variant of Pancreatic Ductal Adenocarcinoma With Distinct CT and MRI Characteristics

Se Jin Choi[1]*, Sung Joo Kim[2]*, Dong Wook Kim[1], Seung Soo Lee[1], Seung-Mo Hong[2], Kyung Won Kim[1], Jin Hee Kim[1], Hyoung Jung Kim[1], Jae Ho Byun[1]

[1]Department of Radiology and Research Institute of Radiology, Asan Medical Center, University of Ulsan College of Medicine, Seoul, Republic of Korea
[2]Department of Pathology, Asan Medical Center, University of Ulsan College of Medicine, Seoul, Republic of Korea

Objective: To investigate the imaging characteristics of large duct pancreatic ductal adenocarcinoma (LD-PDAC) on computed tomography (CT) and magnetic resonance imaging (MRI).

Materials and Methods: Thirty-five patients with LD-PDAC (63.2 ± 9.7 years) were retrospectively evaluated. Tumor morphology on CT and MRI (predominantly solid mass vs. solid mass with prominent cysts vs. predominantly cystic mass) was evaluated. Additionally, the visibility, quantity, shape (oval vs. branching vs. irregular), and MRI signal intensity of neoplastic cysts within the LD-PDAC were investigated. The radiological diagnoses rendered for LD-PDAC in radiology reports were reviewed.

Results: LD-PDAC was more commonly observed as a solid mass with prominent cysts (45.7% [16/35] on CT and 37.1% [13/35] on MRI) or a predominantly cystic mass (20.0% [7/35] on CT and 40.0% [14/35] on MRI) and less commonly as a predominantly solid mass on CT (34.3% [12/35]) and MRI (22.9% [8/35]). The tumor morphology on imaging was significantly associated with the size of the cancer gland on histopathological examination (P = 0.020 [CT] and 0.013 [MRI]). Neoplastic cysts were visible in 88.6% (31/35) and 91.4% (32/35) of the LD-PDAC cases on CT and MRI, respectively. The cysts appeared as branching (51.6% [16/35] on CT and 59.4% [19/35] on MRI) or oval shapes (45.2% [14/35] on CT and 31.2% [10/35] on MRI) with fluid-like MRI signal intensity. In the radiology reports, 10 LD-PDAC cases (28.6%) were misinterpreted as diseases other than typical PDAC, particularly intraductal papillary mucinous neoplasms.

Conclusion: LD-PDAC frequently appears as a solid mass with prominent cysts or as a predominantly cystic mass on CT and MRI. Radiologists should be familiar with the imaging features of LD-PDAC to avoid misdiagnosis.

Keywords: Pancreas; Pancreatic ductal adenocarcinoma; Large duct pancreatic ductal adenocarcinoma; Computed tomography; Magnetic resonance imaging

INTRODUCTION

Pancreatic ductal adenocarcinoma (PDAC), a common pancreatic malignancy with a poor prognosis [1-3], typically appears as a hypovascular solid mass on computed tomography (CT) and magnetic resonance imaging (MRI) [4]. However, cystic changes in PDAC are not uncommon and have been reported in as many as 10% of PDAC cases [5-7]. Cystic changes noted among PDAC cases have been reportedly caused by large cancer glands [6-9]. Bagci et al. [7] introduced the term large duct PDAC (LD-PDAC) to describe this specific morphological variant, which is characterized by cancer glands measuring > 0.5 mm and occupying more than 50% of the tumor. The World Health

Received: May 31, 2023 **Revised:** August 31, 2023 **Accepted:** September 19, 2023
*These authors contributed equally to this work.
Corresponding author: Dong Wook Kim, MD, PhD, Department of Radiology and Research Institute of Radiology, Asan Medical Center, University of Ulsan College of Medicine, 88 Olympic-ro 43-gil, Songpa-gu, Seoul 05505, Republic of Korea
• E-mail: fsnoruen@gmail.com

Korean Journal of Radiology
KJR

Organization (WHO) adopted this classification in the 5th edition of the 'WHO classification of tumours' [10].

Although some studies have reported cystic features on imaging of PDAC [11-14], research on LD-PDAC is lacking, and whether CT or MRI accurately represents the characteristic large cancer glands of LD-PDAC remains uncertain. Given a recent report showing a more favorable outcome for patients with LD-PDAC compared with that of patients with conventional PDAC [15], exploring whether LD-PDAC exhibits distinct imaging characteristics differentiating it from conventional PDAC is important.

Therefore, we aimed to describe the CT and MRI characteristics of pathologically proven LD-PDAC. Additionally, through a retrospective review of radiology reports, we examined whether the LD-PDAC lesions were misdiagnosed, particularly with less aggressive diseases such as pancreatic cystic neoplasms (specifically, intraductal papillary mucinous neoplasms [IPMN]) [16-18], or solid pancreatic tumors with cystic degeneration [19,20].

MATERIALS AND METHODS

This study was approved by the institutional review board of Asan Medical Center (Approval No. 2021-0964), and the requirement for informed consent was waived given the retrospective nature of the study.

Patient Selection

An electronic search of the pathological reports of patients with PDAC treated at a single tertiary institution between January 2014 and January 2021 was performed. We retrospectively enrolled 35 patients (mean age ± standard deviation [SD]: 63.2 ± 9.7 years; 18 males; tumor size: 3.5 ± 1.7 cm) with surgically confirmed LD-PDAC following preoperative CT or MRI (Fig. 1). LD-PDAC was defined as having characteristic large cancer glands measuring > 0.5 mm in diameter or a macroscopically identifiable microcystic growth pattern occupying more than 50% of the total tumor area [7]. For an additional comparative analysis of tumor morphology on imaging and survival, we included 35 patients with conventional PDAC (i.e., PDAC not meeting the LD-PDAC definition) through 1:1 matching with the patients with LD-PDAC based on age, tumor size, and tumor location (mean age ± SD: 63.4 ± 9.9 years; 21 males; tumor size: 3.5 ± 2.3 cm).

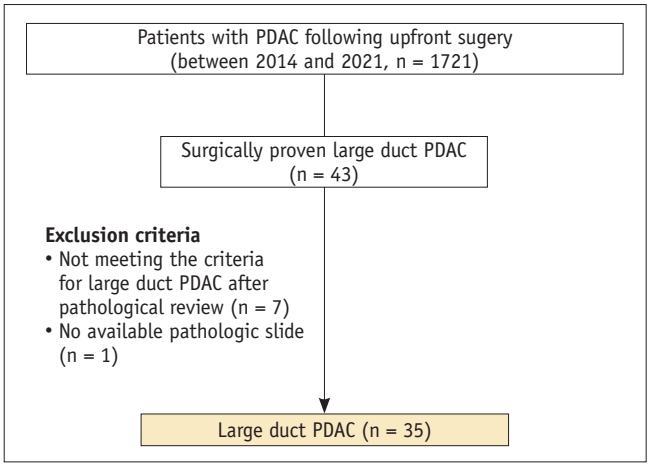

Fig. 1. Flow diagram of the study population. A total of 35 patients with surgically confirmed large duct PDAC were included in our study from 2014 to 2021. PDAC = pancreatic ductal adenocarcinoma

Clinical and Pathological Analysis

Demographic and laboratory data were retrieved from an electronic database. Carbohydrate antigen (CA) 19–9 was obtained within 1 month of resection. Pathologic data, including pathologic TNM staging according to the 8th edition of the American Joint Committee on Cancer staging system [21], resection margin, tumor differentiation, and major vascular, perineural, and lymphovascular invasions, were obtained from the histopathological records of the surgical specimens. Postsurgical progression-free survival (PFS), defined as the time from surgery to disease progression or death, and postsurgical overall survival (OS), defined as the time from surgery to death, were assessed [22]. Patients without disease progression or death were censored at the final follow-up date.

Two board-certified pathologists (S.J.K. and S.M.H., with 4 and 21 years of experience in pancreatic pathology, respectively) performed central histopathological reviews of all surgically resected pancreatic specimens. Pathological characteristics were re-analyzed, including: 1) coexisting IPMN components within the epithelial lining of large cancer glands, 2) the largest size of the cancer glands, 3) the proportion of large cancer glands (defined as the area of large cancer glands larger than 0.5 mm divided by the total tumor area), and 4) the presence of communication with the main pancreatic duct. The pathologists were blinded to all clinical and imaging characteristics.

Imaging Analysis

Imaging protocols for CT and MRI are detailed in

 https://doi.org/10.3348/kjr.2023.0521

Supplementary Method and Supplementary Table 1. The CT and MRI analyses were conducted by two board-certified radiologists (S.J.C. and D.W.K., with 5 and 10 years of experience in abdominal imaging, respectively) who were blinded to the clinical and pathological data. Disagreements between the two readers were resolved by consensus.

The imaging characteristics of the tumors were reviewed, including location, size, margin, CT radiodensity (arterial and portal venous phases), MRI signal intensity on contrast-enhanced T1-weighted imaging (arterial, portal venous, and delayed phases), T2-weighted imaging, and diffusion-weighted imaging. The presence of upstream ductal dilatation and parenchymal atrophy was also evaluated.

Cysts representing large cancer glands visible on CT and MRI (hereafter referred to as neoplastic cysts) were investigated. To differentiate neoplastic cysts from other types (e.g., pseudocysts or retention cysts), only cystic lesions within the imaging boundary of the tumor were included in the imaging analysis. In addition, to exclude intratumoral necrosis and pseudocysts, indeterminate cystic lesions were re-evaluated after they were retrospectively matched with pathological slides. Tumors were categorized according to their morphology on CT and MRI as follows (Fig. 2): 1) predominantly solid mass, defined as visible neoplastic cysts ≤ 10%, 2) solid mass with prominent cysts, defined as 10%–50% visible neoplastic cysts, and 3) predominantly cystic mass, defined as > 50% visible neoplastic cysts.

The visibility, number, shape, and MRI signal intensity of the neoplastic cysts were evaluated. To evaluate which cystic abnormalities the neoplastic cysts resembled, shapes were categorized as: 1) oval (or round; potential mimickers of mucinous cystic neoplasms, serous cystadenoma, and pseudocyst), 2) branching (or tubular; potential mimickers of IPMN), or 3) irregular with a poor margin (potential mimickers of intratumoral necrosis) (Fig. 3) [11,23,24].

Retrospective Review of Imaging Interpretations in Radiology Reports

Radiology CT and MRI reports of patients with LD-PDAC from clinical practice were retrospectively collected from an electronic database. The most likely diagnosis and other possible diagnoses were obtained from the radiology reports.

Statistical Analysis

LD-PDAC tumor morphology on imaging, associated histopathological characteristics, and imaging interpretations were analyzed using one-way analysis of

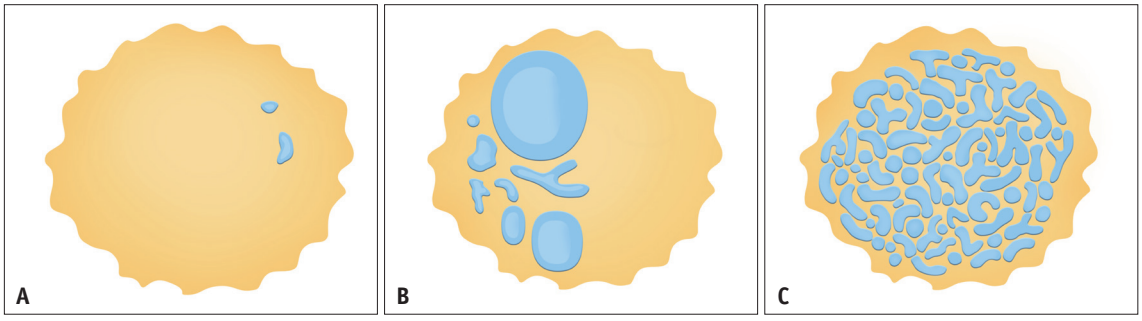

Fig. 2. Morphology of large duct pancreatic ductal adenocarcinoma on CT and MRI. The pancreatic tumors are depicted as yellow masses, while the neoplastic cyst components are colored blue. Predominantly solid mass **(A)**, solid mass with prominent cysts **(B)**, and predominantly cystic mass **(C)**. CT = computed tomography, MRI = magnetic resonance imaging

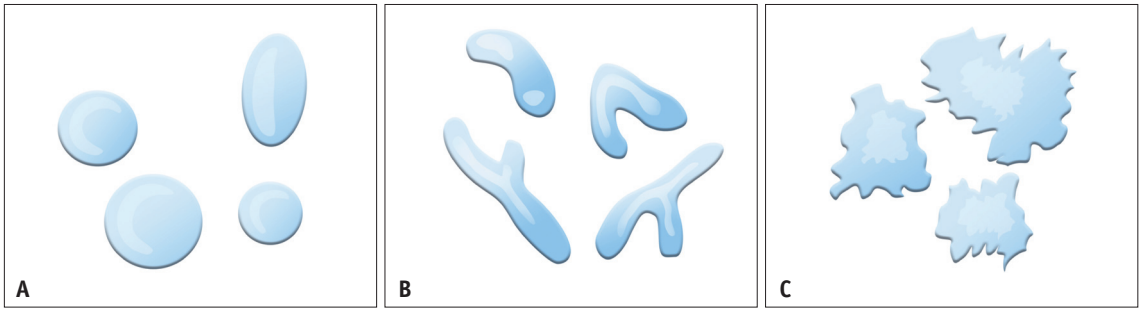

Fig. 3. Neoplastic cyst shapes on CT and MRI. Oval **(A)**, branching **(B)**, and irregular **(C)** with a poor margin. CT = computed tomography, MRI = magnetic resonance imaging

https://doi.org/10.3348/kjr.2023.0521

Korean Journal of Radiology
KJR

variance (ANOVA) and Fisher's exact test, respectively. Inter-reader agreement regarding imaging features of the neoplastic cysts and tumor morphology on CT and MRI was analyzed using Cohen's kappa (κ) and percent agreement. The tumor morphology of the LD-PDAC and conventional PDAC cases on imaging was compared using the chi-square test or Fisher's exact test, as appropriate. Post-surgical OS and PFS were analyzed using the Kaplan-Meier survival curve and compared using the log-rank test. *P* values of < 0.05 were considered statistically significant. Statistical analyses were performed using SPSS software (version 21.0; IBM Corp.) and R software (version 3.6.0; R Foundation for Statistical Computing).

RESULTS

Clinical and Pathological Characteristics

The clinical and pathological characteristics of the patients with LD-PDAC are presented in Table 1. LD-PDAC was most commonly located in the pancreatic head (54.3%), followed by the tail (31.4%) and body (14.3%). Two patients (5.7%) had T1 stage cancer, 25 (71.4%) had T2, and eight (22.9%) had T3. Seventeen patients (48.6%) had regional lymph node metastases (N1 or N2). Eleven tumors (31.4%) were well differentiated, and 24 (68.6%) were moderately differentiated. The mean size of the largest cancer glands was 8.9 mm (SD, ± 5.6 mm). The proportion of cancer glands measuring > 0.5 mm within the tumor cell area ranged from 51.7% to 90% (mean ± SD, 67.5% ± 11.4).

Throughout the follow-up period, 18 patients (51.4%) had postsurgical tumor progression and five patients (14.3%) died. The median post-surgical PFS and OS were 26.3 months and 99.8 months, respectively, indicating significantly extended post-surgical PFS (compared with that at 13.5 months; $P = 0.024$) and post-surgical OS (compared with that at 37.9 months; $P = 0.003$) compared with those of conventional PDAC (Supplementary Fig. 1).

Imaging Characteristics on CT and MRI

The CT and MRI characteristics of the patients with LD-PDAC are shown in Table 2. LD-PDACs typically presented with ill-defined margins (88.6% [31/35] on CT and 82.9% [29/35] on MRI). Furthermore, LD-PDAC exhibited hypo-density or hypo-signal intensity on the arterial phase (93.9% [31/35] on CT and 85.3% [29/35] on MRI), which was less commonly observed on the portal venous phase (80.0% [28/35] on CT and 58.8% [20/35] on MRI) and the delayed phase (38.2% [13/35] on MRI). Patients with LD-PDAC occasionally presented with upstream ductal dilatation (48.6% [17/35] on CT and MRI) and parenchymal atrophy (40.0% [14/35] on CT and 42.9% [15/35] on

Table 1. Clinical and pathologic characteristics

Characteristics	Large duct pancreatic ductal adenocarcinoma (n = 35)
Age, yr	63.2 ± 9.7
Sex, male	18 (51.4)
Body mass index, kg/m^2	22.5 ± 2.5
CA 19–9*, U/mL	67.5 (16.5–127.4)
Size, cm	3.5 ± 1.7
Location	
Head	19 (54.3)
Body	5 (14.3)
Tail	11 (31.4)
Negative resection margin, i.e., R0	29 (82.9)
T stage	
T1	2 (5.7)
T2	25 (71.4)
T3	8 (22.9)
T4	0 (0.0)
N stage	
N0	18 (51.4)
N1	10 (28.6)
N2	7 (20.0)
M stage	
M0	35 (100.0)
Tumor differentiation	
Well differentiated	11 (31.4)
Moderately differentiated	24 (68.6)
Poorly differentiated or undifferentiated	0 (0.0)
Portal vein/superior mesenteric vein invasion	3 (8.6)
Perineural invasion	28 (80.0)
Lymphovascular invasion	13 (37.1)
Coexisting IPMN components	4 (11.4)
Cancer glands	
Largest size, mm	8.9 ± 5.6 (3.0–26.0)
Proportion (%) of cancer glands larger than 0.5 mm	67.5 ± 11.4 (51.7–90.0)
Communication with main pancreatic duct	0 (0)

Unless otherwise indicated, data are mean ± standard deviation with or without range in parentheses for continuous variables and the number with percentage in parentheses for categorical variables.
*Data are median (range).
CA 19-9 = carbohydrate antigen 19-9, IPMN = intraductal papillary mucinous neoplasm

https://doi.org/10.3348/kjr.2023.0521

Table 2. Imaging characteristics of large duct pancreatic ductal adenocarcinoma

Characteristics	CT (n = 35)	MRI (n = 35)
Margin		
Ill-defined	31 (88.6)	29 (82.9)
Well-defined	4 (11.4)	6 (17.1)
Tumor attenuation/signal intensity in arterial phase†		
Iso	2 (6.1)	5 (14.7)
Hypo	31 (93.9)	29 (85.3)
Tumor attenuation/signal intensity in portal venous phase		
Iso	7 (20.0)	14 (41.2)
Hypo	28 (80.0)	20 (58.8)
Tumor/signal intensity in delayed phase‡		
Iso	NA	20 (58.8)
Hypo	NA	13 (38.2)
Upstream duct dilatation	17 (48.6)	17 (48.6)
Upstream parenchymal atrophy	14 (40.0)	15 (42.9)
Diffusion restriction*	NA	27 (79.4)
Neoplastic cysts		
Visibility	31 (88.6)	32 (91.4)
Size, cm	1.4 (0.4–7.1)	1.6 (0.5–7.2)
Number		
0	4 (11.4)	3 (8.6)
1–5	24 (68.6)	20 (57.1)
6–10	1 (2.9)	3 (8.6)
> 10	6 (17.1)	9 (25.7)
Dominant shape		
Oval	14 (45.2)	10 (31.2)
Branching	16 (51.6)	19 (59.4)
Irregular with poor margin	1 (3.2)	3 (9.4)
Tumor morphology		
Predominantly solid mass	12 (34.3)	8 (22.9)
Solid mass with prominent cysts	16 (45.7)	13 (37.1)
Predominantly cystic mass	7 (20.0)	14 (40.0)

Data are number of patients with percentage in parentheses for categorical variables and median with a range in parentheses for neoplastic cyst size.
*Diffusion weighted imaging was obtained in 34 patients, †Arterial phase was obtained in 33 patients, ‡Delayed phase was obtained in 33 patients.
CT = computed tomography, MRI = magnetic resonance imaging, NA = not applicable

MRI). Most (79.4% [27/34]) LD-PDAC cases exhibited diffusion restriction on MRI, although 55.6% (15/27) of the diffusion-restricted LD-PDAC cases did not exhibit restriction within the area of the neoplastic cysts.

Regarding tumor morphology (with an inter-reader agreement of $\kappa = 0.77$ on CT and 0.76 on MRI, as shown in Supplementary Table 2), only 34.3% (12/35) of the LD-PDAC tumors were characterized as predominantly solid masses on CT, and this was less frequently observed on MRI (22.9% [8/35]). These findings are significantly different from those of conventional PDAC, which generally exhibits predominantly solid masses on both CT (100%; $P < 0.001$) and MRI (91.4%; $P < 0.001$) (Supplementary Table 3). In contrast, LD-PDAC often manifested either as a solid mass with prominent cysts in 45.7% (16/35) and 37.1% (13/35) of cases on CT and MRI, respectively (Fig. 4), or as a predominantly cystic mass in 20.0% (7/35) and 40.0% (14/35) of cases on CT and MRI, respectively (Fig. 5).

The tumor morphology of LD-PDAC on CT and MRI was significantly associated with the size of the cancer glands on histopathology ($P = 0.020$ and 0.013, respectively; Table 3) but not with the proportion of cancer glands > 0.5 mm ($P = 0.079$ and 0.400, respectively; Table 3).

The inter-reader agreements regarding the radiological characteristics of the neoplastic cysts are shown in Supplementary Table 2. Neoplastic cysts were visible in most patients with LD-PDAC on both CT (88.6% [31/35]) and MRI (91.4% [32/35]) (Table 2). Neoplastic cyst shapes commonly appeared as either branching (51.6% [16/35] on CT and 59.4% [19/35] on MRI) or oval (45.2% [14/35] on CT and 31.2% [10/35] on MRI), which potentially resembled pancreatic cystic neoplasms (e.g., IPMN, mucinous cystic neoplasms, and serous cystadenoma) or pseudocysts. Approximately 90% of all neoplastic cysts exhibited fluid-like signal intensities on both T2-weighted (90.6% [29/32]) and pre-contrast T1-weighted (93.8% [30/32]) MRI.

Retrospective Review of Imaging Interpretation in Radiology Reports

The imaging interpretations of the 35 cases obtained retrospectively from radiology reports are shown in Supplementary Table 4. LD-PDAC was not directly interpreted as the most likely diagnosis based on imaging in any case. Ten LD-PDAC cases (28.6%) were misinterpreted as diseases other than typical PDAC, including IPMN with or without associated invasive carcinoma (n = 6), solid pseudopapillary neoplasm (n = 2), serous cystadenoma (n = 1), and neuroendocrine neoplasm (n = 1). Those cases misinterpreted as diseases other than typical PDAC were less likely to present as predominantly solid masses (10.0% [1/10] on CT and 0% [0/10] on MRI) than cases interpreted and diagnosed as typical PDAC (36.0% [9/25] on CT and 28.0% [7/25] on MRI; Supplementary Table 5). Additionally, in 40% of the cases (10/25) with the most likely diagnosis of typical PDAC, other diseases were suggested as second possible diagnoses by the radiologists (IPMN with associated invasive carcinoma

https://doi.org/10.3348/kjr.2023.0521

Korean Journal of Radiology
KJR

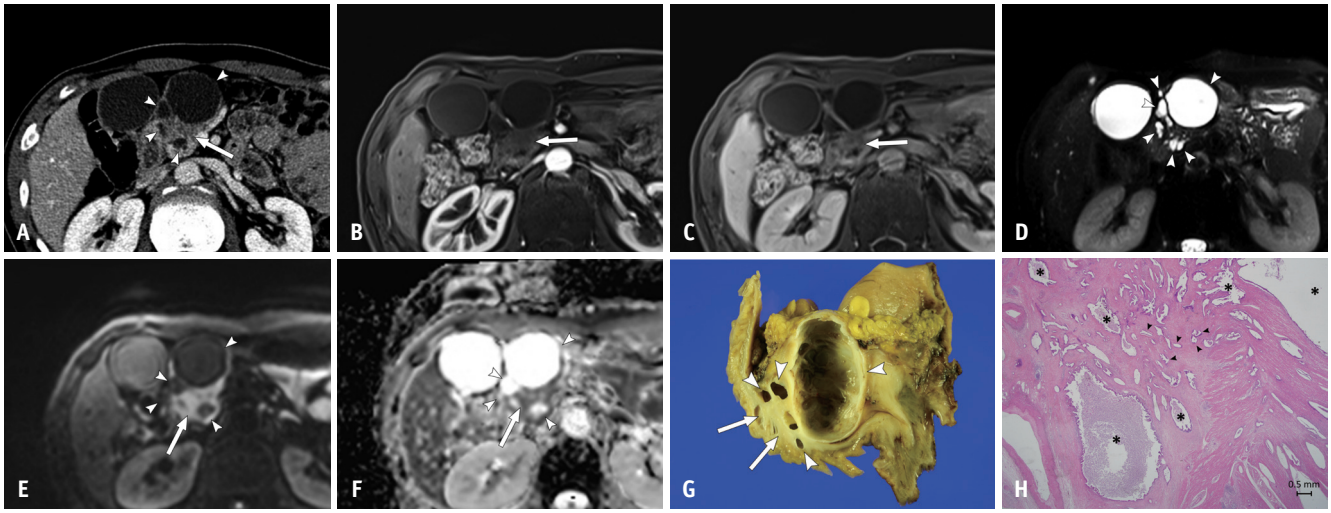

Fig. 4. A 66-year-old male with large duct pancreatic ductal adenocarcinoma which appeared as a solid mass with prominent cysts on CT and MRI. **A:** Portal phase axial contrast-enhanced CT image shows a 5.6-cm hypodense mass (arrow) in the pancreatic head with prominent oval-shaped cysts (arrowheads). **B, C:** Arterial phase axial contrast-enhanced T1-weighted MRI **(B)** shows hypointensity in the solid portion of the tumor (arrows), which is less prominent on delayed phase imaging **(C)**. **D:** Axial T2-weighted MRI identifies more neoplastic cysts with fluid signal intensity (arrowheads) within the mass. **E, F:** Diffusion-weighted (b = 900 s/mm^2) MRI **(E)** and apparent diffusion coefficient map **(F)** depict diffusion restriction in solid parts (arrows) of the tumor whereas no restriction is observed in the cysts (arrowheads). Typical PDAC was the most likely diagnosis; however, mucinous cystic neoplasm was suggested as a possible diagnosis in the radiology report. **G:** The gross surgical specimen shows a 5.1-cm yellowish mass (arrows) with pathologically confirmed neoplastic cysts (arrowheads). **H:** A photomicrograph of the surgical specimen (hematoxylin and eosin stain, x10) reveals multiple neoplastic glands greater than 0.5 mm (asterisks) within the tumor, which may have appeared as cysts on CT and MRI compared with smaller neoplastic glands (arrowheads). PDAC = pancreatic ductal adenocarcinoma, CT = computed tomography, MRI = magnetic resonance imaging

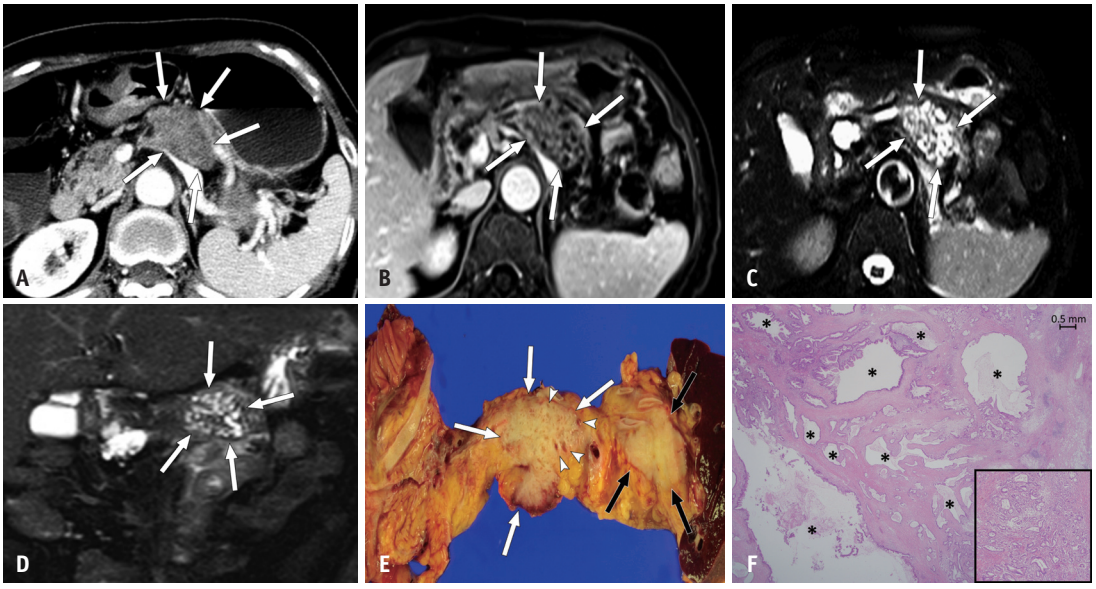

Fig. 5. A 74-year-old female with large duct pancreatic ductal adenocarcinoma. **A:** Portal phase axial contrast-enhanced CT image demonstrates a 5.6-cm predominantly solid mass (arrows) in the pancreatic body without demonstrable cysts. **B, C:** However, the tumor appears as a predominantly cystic mass (arrows) with numerous intratumoral cysts on axial T1-weighted contrast-enhanced **(B)** and T2-weighted **(C)** MRI. **D:** Coronal T2-weighted MRI shows the branching shape of the neoplastic cysts (arrows). The tumor was interpreted as an intraductal papillary mucinous neoplasm in the radiology report. **E:** The gross specimen shows a 5.5 cm yellowish mass (white arrows) in the pancreatic body with visible microcysts (arrowheads), which was confirmed as large duct pancreatic ductal adenocarcinoma. A yellowish mass in the pancreatic tail (black arrows) that was confirmed as conventional pancreatic ductal adenocarcinoma does not have visible microcysts. **F:** A photomicrograph of the surgical specimen (hematoxylin and eosin stain, x10) reveals multiple cancer glands greater than 0.5 mm (asterisks) throughout the tumor, compared with conventional pancreatic ductal adenocarcinoma in the pancreatic tail (inset) composed of small neoplastic glands. CT = computed tomography, MRI = magnetic resonance imaging

https://doi.org/10.3348/kjr.2023.0521

Table 3. Histopathologic features according to tumor morphology of large duct pancreatic cancer on CT and MRI

Histopathology	Morphology				
	Imaging modality	Predominantly solid mass	Solid mass with prominent cysts	Predominantly cystic mass	*P*
Size of the largest cancer glands, mm	CT	4.8 ± 2.8	10.4 ± 6.1	11.1 ± 4.8	0.020
	MRI	3.9 ± 1.2	11.3 ± 6.6	9.0 ± 4.4	0.013
Proportion of cancer glands > 0.5 mm, %	CT	61.1 ± 9.6	69.1 ± 10.5	73.2 ± 13.8	0.079
	MRI	62.4 ± 11.4	68.2 ± 10.2	69.5 ± 12.5	0.400

Data are mean ± standard deviation.
CT = computed tomography, MRI = magnetic resonance imaging

[n = 5], neuroendocrine neoplasm [n = 3], mucinous cystic neoplasm [n = 1], and pancreatitis with pseudocysts [n = 1]).

DISCUSSION

To our knowledge, this study is the first to report CT and MRI characteristics specifically focused on pathologically proven LD-PDAC. Most patients in our cohort with LD-PDAC had visible neoplastic cysts (88.6% [CT] and 91.4% [MRI]), which appeared as branching (51.6% [CT] and 59.4% [MRI]) or oval shapes (45.2% [CT] and 31.2% [MRI]), with fluid-like MRI signal intensities. Thus, LD-PDAC was commonly observed as a solid mass with prominent cysts (45.7% [CT] and 37.1% [MRI]) or as a predominantly cystic mass (20.0% [CT] and 40.0% [MRI]).

Although LD-PDAC shares certain imaging characteristics with PDAC such as ill-defined margins, poor enhancement, and upstream ductal dilation [25], our study revealed a significant prevalence of cystic components within the LD-PDAC masses. Therefore, LD-PDAC cases exhibited distinct imaging features (i.e., a solid mass with prominent cysts or a predominantly cystic mass) that differentiated them from conventional PDAC (i.e., predominantly solid mass). These imaging findings likely reflect the histopathological characteristics of LD-PDAC, which comprises irregularly distributed large cancer glands [7]. Our findings are consistent with those of previous studies that investigated the radiological characteristics of PDAC with prominent neoplastic cysts [11-14], in which the neoplastic cysts varied in sizes (0.5–3.0 cm) and demonstrated fluid-like CT radiodensity or MRI signal intensity [11,12,14]. Kim et al. [13] also reported that PDAC with visible neoplastic cysts is associated with LD-PDAC. Additionally, we found that neoplastic cysts within LD-PDAC typically displayed branching or oval shapes. Branching shapes on CT and MRI may correspond with the microscopic features of irregularly dilated cancer glands [6,7], and oval shapes may depict the honeycomb-like patterns formed by microcysts [6,8].

Due to these imaging characteristics, LD-PDAC could potentially be mistaken for diseases other than PDAC. Our retrospective review of radiology reports revealed that 28.6% of the LD-PDAC cases were misdiagnosed. Importantly, IPMN has emerged as the most relevant differential diagnosis due to its frequent presentation as a cystic mass with tubular or branching morphology on CT and MRI [23,26-28], which is likely attributed to pancreatic ductal dilatation induced by mucin accumulation. In particular, distinguishing colloid carcinoma, a major type of invasive IPMN, from LD-PDAC can be challenging because colloid carcinoma manifests as an ill-defined mass containing heterogeneously dispersed cystic components [29]. Although additional imaging characteristics such as progressive and sponge-like contrast enhancement, multiple amorphous septations, calcification, and communication with and dilatation of the main pancreatic duct [29-31], may serve as essential factors in diagnosing colloid carcinoma and IPMN, further research is required to identify the imaging characteristics that distinguish LD-PDAC from IPMN.

This study had the following limitations. First, the cohort was small. Given that the concept of LD-PDAC has only recently been adopted in clinical practice, certain cases may not have received a specific pathological diagnosis and were excluded from the analysis. Nevertheless, our study sufficiently demonstrated and described the imaging characteristics of LD-PDAC on CT and MRI. Second, we only included patients with LD-PDAC who underwent surgical resection, which could have led to a selection bias. However, this was unavoidable because LD-PDAC should be confirmed exclusively through the analysis of surgical specimens. Third, the surgical specimens were retrospectively reviewed based on photographs of the gross specimens and previously prepared pathology slides; therefore, correlating the size, number, and shape of the cancer gland cysts in the radiology images with those in the pathology slides was difficult. Further prospective studies are

https://doi.org/10.3348/kjr.2023.0521

Korean Journal of Radiology
KJR

required to precisely evaluate the pathological characteristics of LD-PDAC. Fourth, the high misdiagnosis rate (28.6%) in radiologic reports should be interpreted with caution given the relatively recent acceptance of LD-PDAC as a recognized diagnosis in clinical practice.

In conclusion, LD-PDAC presents on CT and MRI as a solid mass with prominent cysts or as a predominantly cystic mass. Radiologists should be familiar with the characteristic imaging features of LD-PDAC to prevent misdiagnosing masses as less aggressive pancreatic diseases, such as IPMN.

Supplement

The Supplement is available with this article at https://doi.org/10.3348/kjr.2023.0521.

Availability of Data and Material

The datasets generated or analyzed during the study are available from the corresponding author on reasonable request.

Conflicts of Interest

Seung Soo Lee, the editor board member of the *Korean Journal of Radiology*, was not involved in the editorial evaluation or decision to publish this article. All authors have declared no conflicts of interest.

Author Contributions

Conceptualization: Dong Wook Kim, Seung Soo Lee. Data curation: Se Jin Choi, Sung Joo Kim, Dong Wook Kim. Formal analysis: Dong Wook Kim. Investigation: Se Jin Choi, Sung Joo Kim, Dong Wook Kim. Methodology: Dong Wook Kim, Seung Soo Lee, Seung-Mo Hong. Supervision: Seung Soo Lee, Seung-Mo Hong. Writing—original draft: Se Jin Choi, Sung Joo Kim, Dong Wook Kim. Writing—review & editing: Seung Soo Lee, Seung-Mo Hong, Kyung Won Kim, Jin Hee Kim, Hyoung Jung Kim, Jae Ho Byun.

ORCID IDs

Se Jin Choi
https://orcid.org/0000-0001-7327-6102
Sung Joo Kim
https://orcid.org/0000-0002-9188-7756
Dong Wook Kim
https://orcid.org/0000-0001-7887-657X
Seung Soo Lee
https://orcid.org/0000-0002-5518-2249
Seung-Mo Hong
https://orcid.org/0000-0002-8888-6007
Kyung Won Kim
https://orcid.org/0000-0002-1532-5970
Jin Hee Kim
https://orcid.org/0000-0001-5036-3326
Hyoung Jung Kim
https://orcid.org/0000-0003-3391-5621
Jae Ho Byun
https://orcid.org/0000-0003-2076-9979

Funding Statement

None

REFERENCES

1. Hartwig W, Werner J, Jäger D, Debus J, Büchler MW. Improvement of surgical results for pancreatic cancer. *Lancet Oncol* 2013;14:e476-e485
2. Siegel RL, Miller KD, Jemal A. Cancer statistics, 2019. *CA Cancer J Clin* 2019;69:7-34
3. Ren B, Liu X, Suriawinata AA. Pancreatic ductal adenocarcinoma and its precursor lesions: histopathology, cytopathology, and molecular pathology. *Am J Pathol* 2019;189:9-21
4. Sahani DV, Shah ZK, Catalano OA, Boland GW, Brugge WR. Radiology of pancreatic adenocarcinoma: current status of imaging. *J Gastroenterol Hepatol* 2008;23:23-33
5. Kosmahl M, Pauser U, Peters K, Sipos B, Lüttges J, Kremer B, et al. Cystic neoplasms of the pancreas and tumor-like lesions with cystic features: a review of 418 cases and a classification proposal. *Virchows Arch* 2004;445:168-178
6. Kosmahl M, Pauser U, Anlauf M, Klöppel G. Pancreatic ductal adenocarcinomas with cystic features: neither rare nor uniform. *Mod Pathol* 2005;18:1157-1164
7. Bagci P, Andea AA, Basturk O, Jang KT, Erbarut I, Adsay V. Large duct type invasive adenocarcinoma of the pancreas with microcystic and papillary patterns: a potential microscopic mimic of non-invasive ductal neoplasia. *Mod Pathol* 2012;25:439-448
8. Hori S, Shimada K, Ino Y, Oguro S, Esaki M, Nara S, et al. Macroscopic features predict outcome in patients with pancreatic ductal adenocarcinoma. *Virchows Arch* 2016;469:621-634
9. Sato H, Liss AS, Mizukami Y. Large-duct pattern invasive adenocarcinoma of the pancreas-a variant mimicking pancreatic cystic neoplasms: a minireview. *World J Gastroenterol* 2021;27:3262-3278
10. WHO classification of tumors editorial board. *Digestive system tumours. WHO classification of tumours series.* 5th ed. Lyon: World Health Organization, 2019:322-332
11. Yoon SE, Byun JH, Kim KA, Kim HJ, Lee SS, Jang SJ, et al.

Pancreatic ductal adenocarcinoma with intratumoral cystic lesions on MRI: correlation with histopathological findings. *Br J Radiol* 2010;83:318-326
12. Hattori Y, Gabata T, Zen Y, Mochizuki K, Kitagawa H, Matsui O. Poorly enhanced areas of pancreatic adenocarcinomas on late-phase dynamic computed tomography: comparison with pathological findings. *Pancreas* 2010;39:1263-1270
13. Kim H, Kim DH, Song IH, Youn SY, Kim B, Oh SN, et al. Identification of intratumoral fluid-containing area by magnetic resonance imaging to predict prognosis in patients with pancreatic ductal adenocarcinoma after curative resection. *Eur Radiol* 2022;32:2518-2528
14. Nitta T, Mitsuhashi T, Hatanaka Y, Hirano S, Matsuno Y. Pancreatic ductal adenocarcinomas with multiple large cystic structures: a clinicopathologic and immunohistochemical study of seven cases. *Pancreatology* 2013;13:401-408
15. Kim SJ, Choi SJ, Yang J, Kim D, Kim DW, Byun JH, et al. Pancreatic ductal adenocarcinoma with a predominant large duct pattern has better recurrence-free survival than conventional pancreatic ductal adenocarcinoma: a comprehensive histopathological, immunohistochemical, and mutational study. *Hum Pathol* 2022;127:39-49
16. Maire F, Hammel P, Terris B, Paye F, Scoazec JY, Cellier C, et al. Prognosis of malignant intraductal papillary mucinous tumours of the pancreas after surgical resection. Comparison with pancreatic ductal adenocarcinoma. *Gut* 2002;51:717-722
17. Poultsides GA, Reddy S, Cameron JL, Hruban RH, Pawlik TM, Ahuja N, et al. Histopathologic basis for the favorable survival after resection of intraductal papillary mucinous neoplasm-associated invasive adenocarcinoma of the pancreas. *Ann Surg* 2010;251:470-476
18. Woo SM, Ryu JK, Lee SH, Yoo JW, Park JK, Kim YT, et al. Survival and prognosis of invasive intraductal papillary mucinous neoplasms of the pancreas: comparison with pancreatic ductal adenocarcinoma. *Pancreas* 2008;36:50-55
19. Halfdanarson TR, Rabe KG, Rubin J, Petersen GM. Pancreatic neuroendocrine tumors (PNETs): incidence, prognosis and recent trend toward improved survival. *Ann Oncol* 2008;19:1727-1733
20. Law JK, Ahmed A, Singh VK, Akshintala VS, Olson MT, Raman SP, et al. A systematic review of solid-pseudopapillary neoplasms: are these rare lesions? *Pancreas* 2014;43:331-337
21. Amin MB, Greene FL, Edge SB, Compton CC, Gershenwald JE, Brookland RK, et al. The Eighth Edition AJCC Cancer Staging Manual: continuing to build a bridge from a population-based to a more "personalized" approach to cancer staging. *CA Cancer J Clin* 2017;67:93-99
22. Punt CJ, Buyse M, Köhne CH, Hohenberger P, Labianca R, Schmoll HJ, et al. Endpoints in adjuvant treatment trials: a systematic review of the literature in colon cancer and proposed definitions for future trials. *J Natl Cancer Inst* 2007;99:998-1003
23. Kim SY, Lee JM, Kim SH, Shin KS, Kim YJ, An SK, et al. Macrocystic neoplasms of the pancreas: CT differentiation of serous oligocystic adenoma from mucinous cystadenoma and intraductal papillary mucinous tumor. *AJR Am J Roentgenol* 2006;187:1192-1198
24. Youn SY, Rha SE, Jung ES, Lee IS. Pancreas ductal adenocarcinoma with cystic features on cross-sectional imaging: radiologic-pathologic correlation. *Diagn Interv Radiol* 2018;24:5-11
25. Schawkat K, Manning MA, Glickman JN, Mortele KJ. Pancreatic ductal adenocarcinoma and its variants: pearls and perils. *Radiographics* 2020;40:1219-1239
26. Lim JH, Lee G, Oh YL. Radiologic spectrum of intraductal papillary mucinous tumor of the pancreas. *Radiographics* 2001;21:323-337; discussion 337-340
27. Procacci C, Graziani R, Bicego E, Bergamo-Andreis IA, Mainardi P, Zamboni G, et al. Intraductal mucin-producing tumors of the pancreas: imaging findings. *Radiology* 1996;198:249-257
28. Muraki T, Jang KT, Reid MD, Pehlivanoglu B, Memis B, Basturk O, et al. Pancreatic ductal adenocarcinomas associated with intraductal papillary mucinous neoplasms (IPMNs) versus pseudo-IPMNs: relative frequency, clinicopathologic characteristics and differential diagnosis. *Mod Pathol* 2022;35:96-105
29. Yoon MA, Lee JM, Kim SH, Lee JY, Han JK, Choi BI, et al. MRI features of pancreatic colloid carcinoma. *AJR Am J Roentgenol* 2009;193:W308-W313
30. Fouladi DF, Raman SP, Hruban RH, Fishman EK, Kawamoto S. Invasive intraductal papillary mucinous neoplasms: CT features of colloid carcinoma versus tubular adenocarcinoma of the pancreas. *AJR Am J Roentgenol* 2020;214:1092-1100
31. Escalon JG, Gerst S, Porembka M, Allen PJ, Do RK. Imaging comparison of tubular and colloid pancreatic adenocarcinoma arising from intraductal papillary mucinous neoplasm on multidetector CT. *Clin Imaging* 2016;40:1195-1199

https://doi.org/10.3348/kjr.2023.0521